

# A Framework for Feature-Centric Filter Design

Gheorghe Craciun\*

Department of Computer and Information Science  
The Ohio State University

David Thompson†

Engineering Research Center for Computational Systems  
Mississippi State University

Raghu Machiraju‡

Department of Computer and Information Science  
The Ohio State University

Yootai Kim§

Department of Computer and Information Science  
The Ohio State University

## Abstract

In this paper we develop a filter design framework emphasizing feature preservation. We are particularly interested in multiscale filters that can be used in wavelet transforms for large datasets generated by computational fluid dynamics simulations. High-fidelity wavelet transforms can facilitate the visualization of large scientific data sets. However, it is important that salient characteristics of the original features be preserved under the transformation. Our effort is different from classical filter design approaches which focus solely on performance in the frequency domain. In particular, we present a set of filter design axioms that ensure certain feature characteristics are preserved and that the resulting filter corresponds to a wavelet transform admitting in-place implementation. We also demonstrate how the axioms can be used to design linear feature-centric filters that are optimal in the sense that they are closest in  $L^2$  to the ideal low pass filter. Results are included that demonstrate the feature-preservation characteristics of each filter.

**Keywords:** Wavelets, Filter Design, TVD, Feature Detection

## 1 Introduction

Large-scale computational fluid dynamics simulations of physical phenomena produce data of unprecedented size (terabyte and petabyte range). Unfortunately, development of appropriate data management and visualization techniques has not kept pace with the growth in size and complexity of such datasets. One paradigm of large-scale visualization is to browse regions containing significant features of the dataset while accessing only the data needed to reconstruct these regions. The cornerstone of an approach of this type is a representational scheme that facilitates ranked access to macroscopic features in the dataset [11, 12, 15]. In this approach, a feature-detection algorithm is used to identify and rank contextually significant features directly in the wavelet domain.

In [11, 12, 15], the linear lifting scheme [18] was used for compressing components of a vector field. The work reported here grew out of our efforts to analyze the implementation of the lifting scheme and design new transforms that more ardently preserve features in discrete flow fields. The rate-distortion characteristics of many wavelet transforms do not bode well for feature preservation [15]. However, it was unclear as to what distortions the wavelet transform wrought on the data. It is therefore useful to evaluate the effect of the wavelet transform in terms of processes that alter the “shape” of the data, i.e., features. Additionally, for very large datasets it is necessary that the feature detection be performed in the

compressed domain. In this context, it is essential that the wavelet transform preserve significant features in the data set.

It is well known that wavelets can efficiently approximate smooth data [5] and produce efficient compression schemes. To suitably preserve edges in scalar image fields, several linear and non-linear or data-dependent schemes have been proposed [13, 6, 7, 4]. In particular, Zhou [24] utilizes Essentially Non-Oscillatory (ENO) reconstructions [9] of the data so that fewer high frequency coefficients are created.

Techniques employed in the study of partial differential equations (PDEs) have been extensively utilized to define the multiscale behavior of feature detection algorithms [1, 10, 16, 22] for images. Typically, the time variable in an evolutionary PDE is taken to represent a scale parameter. In vision and image processing applications, edges can be thought of as discontinuities. These techniques are used to enhance interregion boundaries and smooth intraregion variations. It should be noted that linear PDEs are not completely successful in enhancing boundaries while eliminating noise. Discrete models of the diffusion equation with a nonlinear conductance based on gradient information have proven to be particularly useful for these applications [16, 22].

In this paper we define a framework for the analysis and design of multiscale feature-centric filters through a variational characterization and a multiscale PDE formulation. Given the need for efficient compression and processing, we consider only linear transforms at this time. What is unique about our approach is that we design the behavior of the filter in the spatial domain by appealing to the analysis of an evolutionary partial differential equation. We suggest that the methods proposed here can be used in conjunction with frequency-based methods to design multiscale linear wavelet filters. A result of our three-fold characterization is a set of axioms that can be used to analyze and design filters. Filters that satisfy our axioms will be more likely to preserve features in a linear wavelet space and enable high-fidelity feature detection in large scientific datasets. Additionally, we seek to design filters corresponding to wavelets that can be implemented as a sequence of lifting steps [18].

Our axiomatic filter design resembles the work of Weickert et al. [22] as well as that of Alvarez et al. [2]. Although these efforts yield similar sets of axioms, their frameworks are different since the domain of interest is limited to images populated with strong discontinuities such as edges. In our application, however, not all regions of strong gradients correspond to discontinuities. In fact, features with strong gradients such as expansions and boundary layers should not be treated as discontinuities.

Our paper is structured as follows. We first motivate our effort by considering a simple problem from fluid dynamics that illustrates the effects of applying a standard wavelet transform to the data. Then we consider the general linear filter and describe its evolutionary PDE. We also include an analysis that defines constraints to be placed on the filter coefficients to ensure that new extrema are not created. Next, we formalize our ideas regarding feature preservation. We then present a set of filter design axioms. Using these

\* geraciun@math.ohio-state.edu

† raghu@cis.ohio-state.edu

‡ dst@erc.msstate.edu

§ yootai@cis.ohio-state.edu

axioms, we design linear feature-centric filters that are optimal in the sense that they are closest in  $L^2$  to the ideal low pass filter. Results are included that demonstrate the feature-preservation characteristics of each filter. We stress that our current efforts should be considered as a “work in progress.”

## 2 Motivation

We now provide a simple one-dimensional example from fluid dynamics to provide motivation for this effort. Shown in Figure 1 is a schematic of the shock tube problem. A shock tube can be idealized as a cylinder, closed at both ends, with a diaphragm that separates a region of gas on the left with pressure and density given by  $p_4$  and  $\rho_4$  respectively, from a region of gas on the right with pressure and density given by  $p_1$  and  $\rho_1$ . Note that  $p_4 > p_1$  and  $\rho_4$  must be specified. Initially, the gas is at rest in both regions. The diaphragm is then ruptured instantaneously and an unsteady motion ensues. In a typical situation, four uniform regions and one transitional region emerge. A normal shock wave propagating to the right defines the boundary between uniform Regions 1 and 2. The flow field properties exhibit a nonisentropic, discontinuous change across the moving normal shock. The boundary between Regions 2 and 3 is a contact discontinuity. Density and temperature change discontinuously across the contact discontinuity while pressure and velocity are unchanged. Region 3 is also a uniform region. Region 3 and the uniform Region 4 are separated by an expansion fan in which the flow field properties vary isentropically. Analytical expressions can be used to define the properties in each region under the assumption of one-dimensional inviscid flow. A more complete description of this problem can be found in most compressible fluid dynamics textbooks (e.g., see [3]).

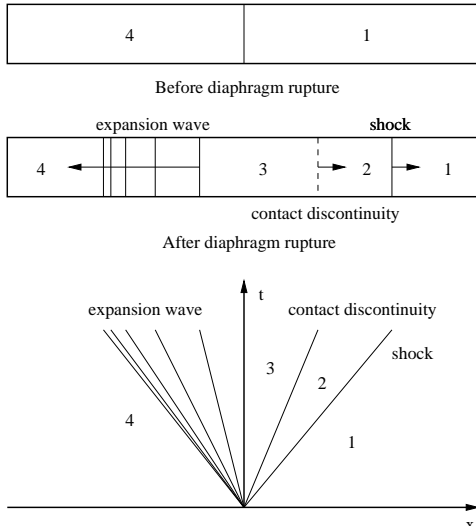


Figure 1: One-Dimensional Shock Tube

Assuming we have a solution to the shock tube problem described above, we now want to visualize the data. In this case, it is not particularly challenging to locate the features in the flow field at a given time. However, for the sake of illustration, we assume that the data set is large and that we want to use a representation scheme that facilitates ranked access to features in the data set as discussed in the introduction. As noted above, a significant component of the process is a feature detection performed using the compressed data. We choose as our wavelet transform the linear lifting scheme [18].

Figure 2 shows a sequence of figures illustrating the effects of applying the linear lifting scheme to the density field of a shock tube solution at a given time. The figure on the top left shows the original data defined using 65 points. Each remaining figure corresponds to an application of the wavelet transform resulting in 33 points, 17 points, and then 9 points. Of particular importance in these figures is the fact that application of the wavelet transform introduces oscillatory behavior in the data. Clearly, these oscillations are unacceptable if a feature detection algorithm based on gradients is to be used. Further, partial reconstruction of the data may be in significant error due to these oscillations and the compression of the otherwise relatively smooth data may not be as efficient.

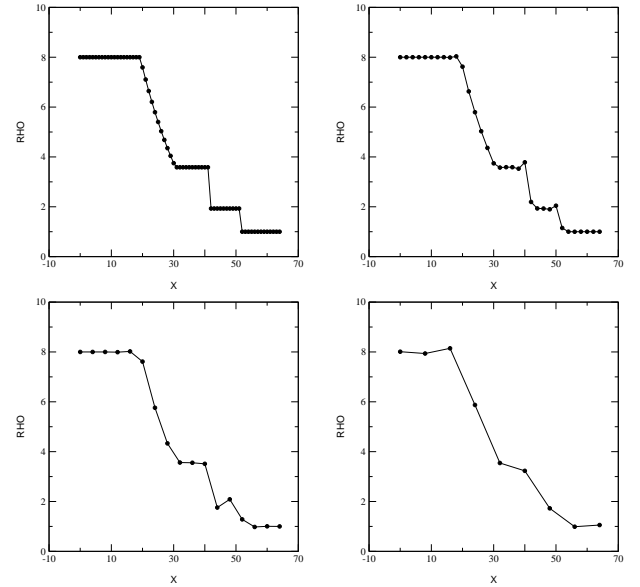


Figure 2: Three Levels of Linear Lifting for Shock Tube Data

## 3 General Linear Filter

We now consider a general linear filter and use an equivalent derived evolutionary PDE to characterize its behavior. We begin by defining a discrete, scalar quantity  $s_{j,l}$  on an equally-spaced mesh  $x_{j,l} = l\Delta x_j$  for  $l = 0, \dots, 2N$  with  $N$  being a positive integer. We seek a multiscale approximation to  $s_{j,l}$  on a second equally-spaced mesh,  $x_{j-1,l} = l\Delta x_{j-1}$  for  $l = 0, \dots, N$  with  $\Delta x_{j-1} = 2\Delta x_j$ , that preserves certain characteristics of the original scalar field. We denote this approximation as  $s_{j-1,l}$ .

We now consider a general linear filter of the form

$$s_{j-1,l} = \sum_{k=-m}^{+n} a_k s_{j,2l+k} \quad (1)$$

where  $m$  and  $n$  are positive integers and the  $a_k$  are constants that are independent of the data. The  $a_k$  are composite coefficients that represent the combined effects of a wavelet transform implemented as a filter. The discrete moments of the filter are given by

$$\alpha_q = \sum_{k=-m}^{+n} k^q a_k . \quad (2)$$

After the filter is applied, the data is subsampled to define the space  $x_{j-1,l}$ .

### 3.1 Evolutionary PDE

We now assume that evolution of the data in the scale space can be thought of as a continuous process and define  $\tau$  to be the continuous scale space variable. Through application of Taylor series expansions in space ( $x$ ) and the scale space ( $\tau$ ), it can be shown [20] that, provided  $\sum_k a_k = 1$ , the application of the linear filter defined in (1) can be thought of as the evolution of the solution to the partial differential equation

$$\begin{aligned} \frac{\partial s}{\partial \tau} &= \alpha_1 \frac{\Delta x_j}{\Delta \tau} \frac{\partial s}{\partial x} + \frac{1}{2!} \frac{\Delta x_j^2}{\Delta \tau} (\alpha_2 - \alpha_1^2) \frac{\partial^2 s}{\partial x^2} \\ &\quad + \frac{1}{3!} \frac{\Delta x_j^3}{\Delta \tau} (\alpha_3 - 3\alpha_1\alpha_2 + 2\alpha_1^3) \frac{\partial^3 s}{\partial x^3} \\ &\quad + \frac{1}{4!} \frac{\Delta x_j^4}{\Delta \tau} (\alpha_4 - 4\alpha_1\alpha_3 - 3\alpha_2 + 12\alpha_1^2\alpha_2 - 6\alpha_1^4) \\ &\quad + \frac{\partial^4 s}{\partial x^4} + O\left(\frac{\Delta x_j^5}{\Delta \tau}\right) \end{aligned} \quad (3)$$

with the initial data given as the original discrete data  $s_{j,l}$ . Note that the evolution of the scalar  $s$  in (3) depends explicitly on the sampling rate  $\Delta x_j$ . Also, we are not interested in the limiting behavior as  $\Delta x \rightarrow 0$  and  $\Delta \tau \rightarrow 0$  since the filter (1) is implemented only on discrete data, i.e., for finite values of  $\Delta x$ .

In this context, the behavior of the data in the spatial domain upon application of the general filter (1) is equivalent to the behavior of the solution of the evolutionary PDE (3). This approach is based to the modified equation analysis [21] used in computational fluid dynamics. An analysis of spatial filters using Taylor series expansions was described in [14] where the filter performance was described in terms of spatial criteria by examining the non-zero discrete moments, i.e., the  $\alpha_q$  in (2).

### 3.2 Frequency Response

The frequency response or amplification factor of the filter is given by

$$G(\beta) = \sum_{k=-m}^{+n} a_k e^{ik\beta} \quad (4)$$

where the amplification factor represents the response for the frequency  $\beta$ . The magnitude of  $G(\beta)$  measures the amplitude of a unit Fourier coefficient upon application of the filter and the phase of  $G(\beta)$  measures the phase shift that occurs after application of the filter.

### 3.3 TVD Constraints

The  $a_k$  values can be restricted by appealing to another concept from computational fluid dynamics. In CFD simulations, great effort is expended to ensure that the numerical scheme not introduce artificial extrema in the solution. In modern CFD simulations, nonlinear techniques typically called “limiting” are used with some success to achieve higher-order temporal and spatial accuracy without spurious oscillations. Harten [8] and Yee [23] have made significant contributions to this field with their work on Total Variation Diminishing (TVD) algorithms. In a TVD algorithm, the total variation of the solution does not increase with time, or

$$TV(s^{n+1}) \leq TV(s^n) \quad (5)$$

where  $s^n$  is the solution at the current time level,  $s^{n+1}$  is the solution at the next time level, and the total variation of the solution is

given by

$$TV(s) = \sum_{-\infty}^{+\infty} |s_{l+1} - s_l| \quad (6)$$

where  $s_{l+1}$  and  $s_l$  are spatially consecutive values of the solution. By limiting the total variation of the solution to be less than or equal to the value in the initial data, spurious oscillations do not develop in the data. In vision literature, this condition is often achieved through the imposition of causality condition [16].

We now want to impose the condition that the total variation of the data not increase as we proceed from finer to coarser scales. Further, let us notice that we are actually just interested in the subsampled data  $s_j$  to be TVD. We will now describe a necessary and sufficient condition for this to hold for any values of  $s_j$ .

Let us first look at the special case where the  $2N$  values of  $s_j$  on level  $j$  are of the form  $0, 0, \dots, 0, 1, 1, \dots, 1$ . Without loss of generality we can suppose that  $a_k = 0$  for all  $k \leq 0$  and for all  $k > n+1$ . For large enough values of  $N$  the intermediate values  $\bar{s}_j$  will have the form  $0, 0, \dots, 0, a_n, a_n + a_{n-1}, a_n + a_{n-1} + a_{n-2}, \dots, a_n + \dots + a_1, a_n + \dots + a_1, \dots, a_n + \dots + a_1$ . (Here we supposed that we use an appropriate method of handling the boundary when computing the convolution product, by which the input signal  $s_j$  is padded at each boundary with values representing the average values near that boundary.) Therefore the subsampled data  $s_{j-1}$  will have either the form  $0, 0, \dots, 0, a_n, a_n + a_{n-1} + a_{n-2}, a_n + a_{n-1} + a_{n-2} + a_{n-3} + a_{n-4}, \dots, a_n + \dots + a_1, a_n + \dots + a_1, \dots, a_n + \dots + a_1$ , or the form  $0, 0, \dots, 0, a_n + a_{n-1}, a_n + a_{n-1} + a_{n-2} + a_{n-3}, \dots, a_n + \dots + a_1, a_n + \dots + a_1, \dots, a_n + \dots + a_1$ . From this it follows that either

$$TV(s_{j-1}) = \sum |a_{2k} + a_{2k+1}| \quad (7)$$

or

$$TV(s_{j-1}) = \sum |a_{2k-1} + a_{2k}| \quad (8)$$

according to the parity of the index  $l$  such that  $s_{j,l} = 0$  and  $s_{j,l+1} = 1$ . Let us notice that  $TV(s_j) = 1$ . This implies that a necessary condition for  $TV(s_{j-1}) \leq TV(s_j)$  is that the coefficients in Equation 1 satisfy the following two inequalities

$$\begin{aligned} \sum |a_{2k} + a_{2k+1}| &\leq 1 \\ \sum |a_{2k-1} + a_{2k}| &\leq 1 \end{aligned} \quad (9)$$

We will now prove that the two inequalities (9) are also a sufficient condition for  $TV(s_{j-1}) \leq TV(s_j)$ . Without loss of generality we can suppose  $s_{j,k} = 0$  for all  $k < 0$ . For some fixed level  $j$  and values  $s_j$  let us define  $y$  by

$$y_k = s_{j,k+1} - s_{j,k} \quad (10)$$

Also, let us consider a matrix  $A$  with components  $A_{m,i} = a_{i-2m-1} + a_{i-2m-2}$ . Recall that  $|A|_1 = \max_i \sum_m |A_{m,i}|$ , where  $|\cdot|_1$  is the usual  $L^1$  operator norm. If (9) holds, then we have

$$\sum_m |A_{m,i}| \leq 1 \quad (11)$$

for any  $i$ , which implies that  $|A|_1 \leq 1$ . In particular, it follows that  $|Ay|_1 \leq |A|_1 |y|_1 \leq |y|_1$ , so

$$\sum_m |\sum_i A_{m,i} y_i| \leq \sum_m |y_m| \quad (12)$$

We are now going to show that the desired inequality  $TV(s_{j-1}) \leq TV(s_j)$  is implied by (12). We have

$$TV(s_{j-1}) = \sum_m |\bar{s}_{j,2m+2} - \bar{s}_{j,2m}| \quad (13)$$

$$\begin{aligned}
&= \sum_m \left| \sum_i a_i s_{j,2m+2+i} - \sum_i a_i s_{j,2m+i} \right| \\
&= \sum_m \left| \sum_i a_i (s_{j,2m+2+i} - s_{j,2m+i}) \right| \\
&= \sum_m \left| \sum_i a_i (y_{2m+i+2} + y_{2m+i+1}) \right|
\end{aligned}$$

On the other hand according to (12) we have

$$\begin{aligned}
TV(s_j) &= \sum_m |s_{j,m+1} - s_{j,m}| \\
&= \sum_m |y_m| \\
&\geq \sum_m \left| \sum_i A_{m,i} y_i \right| \\
&= \sum_m \left| \sum_i (a_{i-2m-1} + a_{i-2m-2}) y_i \right|
\end{aligned} \tag{14}$$

Let us also notice that

$$\sum_i a_i (y_{2m+i+2} + y_{2m+i+1}) = \sum_i (a_{i-2m-1} + a_{i-2m-2}) y_i \tag{15}$$

Finally by putting (13), (14), and (15) together we get  $TV(s_{j-1}) \leq TV(s_j)$ . Therefore we have proved that (9) is a necessary and sufficient condition for  $TV(s_{j-1}) \leq TV(s_j)$ . Let us also notice that in the special case when  $\sum a_i = 1$ , i.e. the coefficients  $a_i$  are a partition of unity, we can use the inequalities

$$\begin{aligned}
\sum |a_{2k} + a_{2k+1}| &\geq \sum a_k \\
\sum |a_{2k-1} + a_{2k}| &\geq \sum a_k
\end{aligned} \tag{16}$$

to conclude that the condition (9) is equivalent to having

$$a_i + a_{i+1} \geq 0 \tag{17}$$

for all  $i$ . In other words, in the partition of unity case, a necessary and sufficient condition for  $TV(s_{j-1}) \leq TV(s_j)$  for any  $s_j$  is that for all negative  $a_i$  the inequalities  $|a_i| \leq a_{i-1}$  and  $|a_i| \leq a_{i+1}$  hold.

### 3.4 The Lifting Scheme

The lifting scheme is a method of factoring wavelet filters into basic building blocks called lifting steps, which also allows for spatial domain wavelet design [19]. Each lifting step consists of three parts: split, predict, and update. This means that we first split the input sequence into even and odd entries. Then we predict the odd values based on the even values and replace them with the differences between actual values and the predictions. These values then become the detail coefficients. The even values are then updated using these detail coefficients so as to maintain certain global properties. Daubechies and Sweldens also showed that every FIR wavelet or filter bank can be decomposed into lifting steps [19]. Moreover, lifting allows for an in-place implementation of the wavelet transform and leads to an improvement in efficiency when compared to the standard implementation.

## 4 Feature Preservation

It is now appropriate to define what we mean by feature preservation. In this context, feature preservation implies that the “location”, “shape”, and “strength” of features are unchanged after the

application of the general filter (1). Of course, differences naturally occur due to the change in resolution between  $x_{j,l}$  and  $x_{j-1,l}$ . We now state these ideas in more concrete terms.

- The “location” of a feature is simply its position within the domain. As discussed in [20], odd order derivative terms in the evolutionary PDE (3) correspond to a convection or translation of features in the domain. If the filter is symmetric,  $a_k = a_{-k}$  for all  $k$ , the coefficients multiplying the convective terms are identically zero and no translation of the data occurs.
- The “shape” of a feature can be described in terms of regions of monotone variation in the data. For the “shape” to be preserved, the linear filter should not introduce new extrema. This condition is expressed in [16] as the “causality condition.” This condition can be imposed by ensuring that the linear transform is Total Variation Diminishing (TVD) after the data is subsampled, i.e. 17,  $a_k + a_{k+1} \geq 0$  for all  $k$  provided  $\sum_k a_k = 1$ .
- The “strength” of a feature can be described in terms of the changes in the data. For the strength to be preserved, the linear filter should not accentuate or diminish local extrema. This condition can be related to the frequency response (4) of the filter. Our evolutionary PDE framework (3) characterizes changes in feature strength in terms of the even order derivative terms which represent the diffusive tendencies of the filter.

## 5 Axioms

Having defined feature preservation, we now enumerate a list of filter design axioms. We want to formulate a set of requirements on the coefficients  $a_k$  that can guide the design of a wavelet transform associated with the coefficients  $a_k$  in addition to preserving features. We define the *restricted transfer operator*  $T$  as follows: if the length of the convolution product of the sequence of coefficients  $a_k$  with itself is  $N$ , then  $T$  is the  $(N-2) \times (N-2)$  matrix obtained from double shifts of this convolution product, times 2 (see [17]). Let us impose the following requirements on the coefficients  $a_k$ :

- (R1)  $\sum_k a_k = 1$
- (R2)  $\sum_k (-1)^k k^j a_k = 0$ , for  $j = 0, 1, \dots, p-1$ , and some  $p \geq 1$
- (R3) the restricted transfer operator  $T$  has one eigenvalue  $\lambda = 1$ , and all other eigenvalues have  $|\lambda| < 1$
- (R4)  $a_k + a_{k+1} \geq 0$  for all  $k$
- (R5)  $a_k = a_{-k}$  for all  $k$
- (R6) if  $a_{-n}$  is the first nonzero coefficient, then the polynomials  $a_{-n} + a_{-n+2}z + a_{-n+4}z^2 + \dots$  and  $a_{-n+1} + a_{-n+3}z + a_{-n+5}z^2 + \dots$  are relatively prime.
- (R7) between all filters with the desired properties, the filter given by the coefficients  $a_k$  minimizes the  $L^2$  distance to the *sinc* filter.

Axioms (R1), (R4), and (R5) are related to the feature preservation properties of the filter. Axiom (R2) dictates the performance of the frequency response at  $\beta = \pi$ . Axioms (R3) and (R6) ensure

that the proposed filter is the low pass filter of a wavelet transform which can be implemented as a series of lifting steps. Axiom (R7) minimizes blurring and aliasing. It should be noted that the coefficients for the *sinc* filter do not satisfy the TVD constraint (17). Thus, any filter design strategy will seek a compromise between the ideal frequency behavior and the feature preservation properties of TVD filters.

**Theorem.** Requirements (R1)-(R7) are necessary and sufficient conditions for the following properties to hold:

- (a) (Convergence of the cascade algorithm, see [17])  
The iteration  $\phi^{(i+1)}(t) = \sum_k 2a_k \phi^{(i)}(2t - k)$ , where  $\phi^{(0)}$  is a box function, converges in  $L^2$ .
- (b) (Accuracy of approximation of order  $p$ )  
The error estimate for a function  $f(t)$  of class  $C^p$  at scale  $\Delta t = 2^{-j}$  is of the form  $C(\Delta t)^p |f^{(p)}(t)|$ .
- (c) (Total variation diminishing from finer to coarser scales)  
 $TV(s_{j-1}) \leq TV(s_j)$ .
- (d) (Zero phase shift from finer to coarser scale)  
In the evolutionary PDE (3), all coefficients multiplying even order derivatives are zero.
- (e) (Lifting scheme implementation, see [19])  
There exists complementary high-pass filter, and the associated wavelet transform admits in-place implementation using the lifting scheme.
- (f) (Average grey level invariance)  
The average of the data is unchanged when passing from finer to coarser scales.
- (g) (Preservation of low frequencies)  
The moment of order 0 is 1, and the moment of order 1 is 0.
- (h) (Optimality)  
Between all filters with the desired properties, the filter given by the coefficients  $a_k$  minimizes the  $L^2$  distance in the frequency domain to the ideal brick wall filter.

Properties (a) – (h) are related to (R1) – (R7) as follows: (a) is equivalent to (R3), (b) is equivalent to (R2), (c) is implied by (R1) and (R4), (d) is implied by (R5), (e) is equivalent to (R6), (f) is equivalent to (R1), (g) is implied by (R1) and (R5), and (h) is equivalent to (R7).

## 6 Filter Design

We now use the framework developed in the previous sections to design feature-centric filters. For a symmetric filter with coefficients  $a_k$  the frequency response (4) takes the form:

$$G(\beta) = a_0 + 2 \sum_{k \geq 1} a_k \cos(k\beta) \quad (18)$$

Then all derivatives of  $G$  of odd order vanish at zero and at  $\pi$ . Therefore it is enough for  $G(\beta)$  to have, for example, the second derivative at  $\pi$  equal to zero, and then its first, second and third derivatives at  $\pi$  are zero.

Let us examine the the symmetric TVD filters with two zeros at  $\pi$  that, for a given length  $N$ , are closest in  $L^2$  to the ideal low pass

filter. To compute them, we consider the square of the norm of the difference between our filter and the ideal low pass filter, subject to the TVD inequalities, and to the two linear identities given by (R1) and (R2). Then we have to minimize a quadratic function of  $a_0, \dots, a_n$  subject to some linear inequalities and identities. We can replace the TVD inequalities with positivity requirements by using the following linear substitution:

$$\begin{aligned} a_n &= b_n \\ a_{n-1} &= b_{n-1} - b_n \\ a_{n-2} &= b_{n-2} - b_{n-1} + b_n \\ &\dots \\ a_0 &= b_0 - b_1 + b_2 - \dots (-1)^n b_n \end{aligned} \quad (19)$$

This allows us to reduce the problem to minimizing a quadratic function subject to some linear identities on the positive domain. Moreover, we can restrict the domain further to the cube  $[0, 1] \times [0, 1] \times \dots \times [0, 1]$ , when we notice that the TVD conditions imply that  $b_k \leq 1$  for any  $k$ . This allows us to use a recursive procedure to compute the *exact* values of the solutions. We list the resulting  $a_k$ 's just for  $k \geq 0$ , because for  $k < 0$  they are determined by symmetry:

$N$	coeff	value
3	$a_0$	1/2
	$a_1$	1/4
5	$a_0$	1/2
	$a_1$	1/4
	$a_2$	0
7	$a_0$	1/2
	$a_1$	1/4
	$a_2$	0
	$a_3$	0
9	$a_0$	$(21\pi - 16)/36\pi$
	$a_1$	$(33\pi + 16)/144\pi$
	$a_2$	$(16 - 3\pi)/144\pi$
	$a_3$	$-(16 - 3\pi)/144\pi$
	$a_4$	$(16 - 3\pi)/144\pi$
11	$a_0$	$(375\pi - 224)/690\pi$
	$a_1$	$(165\pi + 608)/1380\pi$
	$a_2$	$(112 - 15\pi)/1380\pi$
	$a_3$	$-(112 - 15\pi)/1380\pi$
	$a_4$	$(112 - 15\pi)/1380\pi$
	$a_5$	$(165\pi - 496)/1380\pi$

We can notice that all these optimal filters are actually very close to  $(1/4, 1/2, 1/4)$ , even if we allow a large number of taps. Also, we observed that when the number of taps  $N$  is larger than 11 the solution remains the same as in the case  $N = 11$ .

Let us look now at symmetric TVD filters with four zeros at  $\pi$  that are also closest to the ideal low pass filter. Again, we minimize the quadratic function given by the square of the norm of the difference between our filter and the ideal low pass filter, subject to the TVD inequalities, and to three linear identities, one given by (R1) and two given by (R2). We get:

$N$	coeff	value
5	$a_0$	3/8
	$a_1$	1/4
	$a_2$	1/16
7	$a_0$	3/8
	$a_1$	1/4
	$a_2$	1/16
	$a_3$	0
9	$a_0$	13/28
	$a_1$	29/112
	$a_2$	1/112
	$a_3$	-1/112
	$a_4$	1/112
11	$a_0$	$(-288 + 1075\pi)/2230\pi$
	$a_1$	$(-192 + 9265\pi)/35680\pi$
	$a_2$	$(5\pi + 36)/1115\pi$
	$a_3$	$-(5\pi + 36)/1115\pi$
	$a_4$	$(5\pi + 36)/1115\pi$
	$a_5$	$(1344 - 185\pi)/35680\pi$

We can notice that, as we increase the number of taps, the solution approaches a value which is very close to the value in the previous table.

If we try to increase *both* the number of zeros at 0 and the number of zeros at  $\pi$  while imposing the TVD inequalities, we will notice that there are no nontrivial solutions. For example, if the second derivative of  $G(\beta)$  has the property  $G''(0) = G''(\pi) = 0$ , then we get:

$$a_1 + 4a_2 + 9a_3 + 16a_4 + 25a_5 + \dots$$

$$= a_1 - 4a_2 + 9a_3 - 16a_4 + 25a_5 - \dots = 0$$

From this we conclude that:

$$a_1 + 9a_3 + 25a_5 + \dots = 4a_2 + 16a_4 + 36a_6 + \dots = 0,$$

and then

$$(a_1 + a_2) + 3(a_2 + a_3) + 6(a_3 + a_4) + 10(a_4 + a_5) + \dots = 0$$

which together with the TVD inequalities implies that

$$a_1 + a_2 = a_2 + a_3 = a_3 + a_4 = a_4 + a_5 = \dots = 0$$

and this together with the filter being FIR implies that  $a_k = 0$  for all  $k \geq 1$ . The same holds if we replace the second derivative above with any other even order derivative of  $G(\beta)$ .

We can also look at symmetric TVD filters which have the maximum number  $p$  of zeros at  $\pi$ . For any  $N$  we solve a system of linear inequalities given by the TVD conditions, and identities given by the equations (R2) for the maximum  $p$  for which a solution still exists. We get:

$N$	$p$	coeff	value
3	2	$a_0$	1/2
		$a_1$	1/4
5	4	$a_0$	3/8
		$a_1$	1/4
		$a_2$	1/16
		$a_3$	
7	6	$a_0$	5/16
		$a_1$	15/64
		$a_2$	3/32
		$a_3$	1/64
		$a_4$	
9	8	$a_0$	35/128
		$a_1$	7/32
		$a_2$	7/64
		$a_3$	1/32
		$a_4$	1/256
		$a_5$	
11	10	$a_0$	63/256
		$a_1$	105/512
		$a_2$	15/128
		$a_3$	45/1024
		$a_4$	5/512
		$a_5$	1/1024

The filters above are the TVD filters that give the smallest order error estimate for smooth data, while also preserving low frequencies, and annihilating high frequencies.

## 7 Results

Let us describe a complete filter bank associated to the symmetric TVD filter  $h = (1/4, 1/2, 1/4)$ . According to [19] there exist many complementary high pass filters associated to a given low pass filter. Let us look for a symmetric one. It is easy to check that the best we can do with a two-step lifting is  $g = (-1/8, -1/4, 3/4, -1/4, -1/8, 0, 0)$ . It is not possible for  $g$  to be symmetric, but the one above has linear phase, and is the shortest complementary filter with these properties. The filters  $h$  and  $g$  form the analysis half of the filter bank. To get a biorthogonal wavelet transform the associated synthesis filters will have to be  $h^{\sim} = (-1/8, 1/4, 3/8, 1/4, -1/8)$ , and  $g^{\sim} = (0, 0, -1/4, 1/2, -1/4)$ . This is the dual of the biorthogonal Cohen-Daubechies-Feauveau (5,3) wavelet system (we thank Dr James Fowler for pointing out this relationship to us).

Figure 3 shows the same sequence of images shown in Figure 2 using the TVD filter. Unlike Figure 2, the initially monotone data remains monotone. Although the dissipative nature of the filter is evident from some smearing (blurring) of the features, the dissipation of the filter is not too severe. Higher-order filters may well provide some improvement in this regard.

Let us look at what happens when we use TVD and non-TVD wavelet transforms to compress two dimensional data. The compressed images in Figure 5 and Figure 6 are obtained from the same shockwave image in Figure 4. The image in Figure 5 was compressed using the wavelet transform associated to the symmetric TVD filter (1/4, 1/2, 1/4), while the images in Figure 6 were compressed using the cubic wavelet, which is not TVD (see [20]). We notice that all the images compressed using the cubic wavelet have strong artifacts due to the sharp variation near discontinuities.

Let us also look at a three dimensional data set. In Figure 7 we have an explosion data set, and we again apply TVD and cubic wavelet transforms. The result is that in the image obtained from the non-TVD wavelet transform brightness is significantly reduced, since the surface of the transformed body loses its smoothness.

## 8 Conclusions

In this paper we defined a framework for the analysis and design of multiscale filters through a variational characterization and a multiscale PDE formulation. Included in this framework are a set of axioms that can be used to design filters that preserve certain characteristics of the data—namely the position, shape, and strength of features.

We suggest that the methods proposed here can be used in conjunction with frequency-based methods to design multiscale linear wavelet filters. We plan to utilize these techniques to develop advanced wavelets with feature-preserving qualities.

## 9 Acknowledgments

This work is partially funded by the NSF under the Large Data and Scientific Software Visualization Program (ACI-9982344) and an NSF Early Career Award (ACI-9734483). We would also like to thank Ming Jiang for his help coding the wavelet transforms.

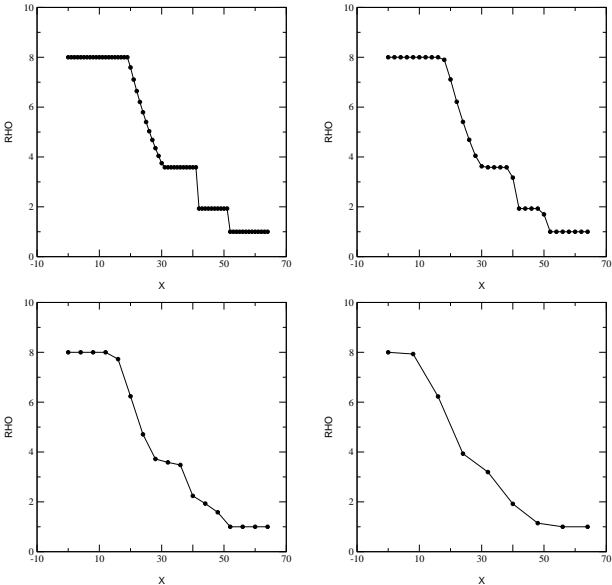


Figure 3: Three Levels of TVD Lifting for Shock Tube Data

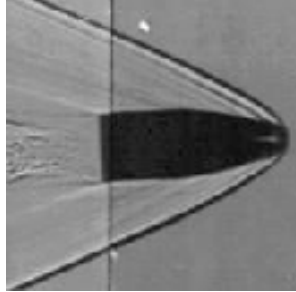


Figure 4: Original 2d shock image

## References

- [1] Special Issue on Partial Differential Equations and Geometry-Driven Diffusion. *IEEE Trans. Image Proc.*, 7, 1998.
- [2] L. Alvarez, F. Guichard, P. L. Lions, and J. M. Morel. Axioms and fundamental equations of image processing. *Arch. Rational Mech. Anal.*, 16(9):199–257, 1993.
- [3] J. D. Anderson. *Modern Compressible Flow with Historical Perspective*. McGraw Hill, 1982.
- [4] P. Claypoole, G. Davis, W. Sweldens, and R. Baraniuk. Non-linear wavelet transforms for image coding. In *Asilomar Conference on Systems, Signals and Computers, (preprint)*, 1997.
- [5] I. Daubechies. *Ten Lectures on Wavelets*. SIAM, 1992.
- [6] D. Donoho. Denoising by soft thresholding. *IEEE Trans. Inf. Theory*, 41:613–627, 1995.
- [7] D. Donoho, I. Daubechies, R. DeVore, and M. Vetterli. Adapting to unknown smoothness via wavelet shrinkage. *J. Amer. Stat. Assoc.*, 90:1200–1224, 1995.
- [8] A. Harten. On a class of high resolution total-variation-stable finite-difference schemes. *SIAM J. Num. Anal.*, 21:1–23, 1984.
- [9] A. Harten, E. Enquist, S. Osher, and S. Chakravarthy. Uniformly high order essentially non-oscillatory scheme, III. *J. Comp. Phys.*, 71:231–303, 1987.
- [10] B. Kimia, A. Tannenbaum, and S. W. Zucker. Towards a computational theory of shape. *Lect. Notes Comp. Sci.*, 427, 1990.
- [11] R. Machiraju, J. Fowler, D. Thompson, W. Schroeder, and B. Soni. EVITA - Efficient visualization and interrogation of tera-scale data. In *Data Mining for Scientific and Engineering Applications (to appear)*, 2001.
- [12] R. Machiraju, B. Nakshatrala, , and D. Thompson. Feature-based ranked representation of vector fields. In *Proc. of Dagstuhl 2000 Seminar on Scientific Visualization (submitted)*, 2001.
- [13] S. Mallat. *A Wavelet Tour of Signal Processing*. Academic Press, 1998.
- [14] T. Möller, R. Machiraju, K. Mueller, and R. Yagel. Evaluation and design of optimal filters using a Taylor series expansion. *IEEE Trans. Vis. Graphics*, 3:184–199, 1997.
- [15] B. Nakshatrala. Feature-based embedded representation of vector fields. Master’s thesis, Mississippi State University, December 1999.
- [16] P. Perona and J. Malik. Scale-space diffusion and edge detection using anisotropic diffusion. *IEEE Trans. Pat. Anal. Int.*, 12:629–639, 1990.
- [17] G. Strang and T. Nguyen. *Wavelets and Filter Banks*. Wellesley-Cambridge Press, 1996.
- [18] W. Sweldens. The lifting scheme: A construction of second generation wavelets. *SIAM J. Math. Anal.*, 29:511–526, 1997.
- [19] W. Sweldens and I. Daubechies. Factoring wavelet transforms into lifting steps. *J. Fourier Anal. Appl.*, 29:511–546, 1997.
- [20] D. Thompson, R. Machiraju, G. Craciun, and M. Jiang. Feature preservation properties of linear wavelet transforms (submitted). In *Proc. Yosemite Multiscale Multiresolution Symp.*, Yosemite, CA, 2000.
- [21] R. F. Warming and B. J. Hyett. The modified equation approach to the stability and accuracy analysis of finite-difference methods. *J. Comp. Phys.*, 14:159–179, 1974.

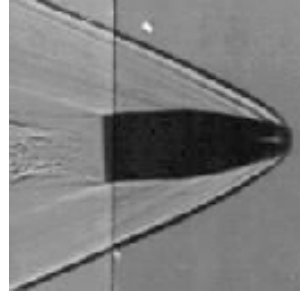
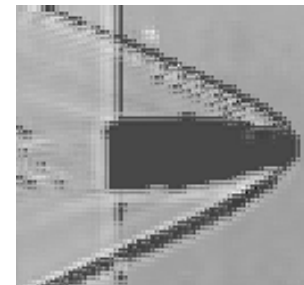
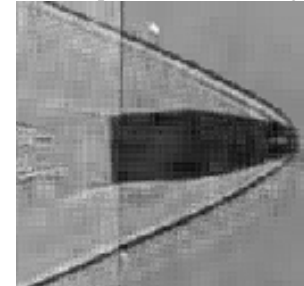


Figure 5: TVD lifting - 2d shock image (20% compression and 2 lifting steps)

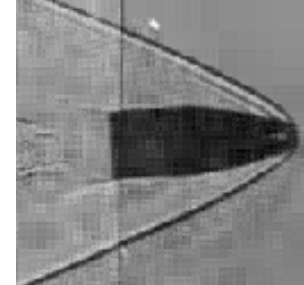
- [22] J. Weickert, B. M. ter Haar Romeny, and M. A. Viergever. Efficient and reliable schemes for nonlinear diffusion filtering. *IEEE Trans. Image Proc.*, 7(3):398–410, March 1998.
- [23] H. C. Yee. A class of high-resolution explicit and implicit shock-capturing methods. NASA TM 101088, NASA Ames Research Center, February 1989.
- [24] H.-M. Zhou. *Wavelet transforms and pde techniques in image compression*. PhD thesis, University of California Los Angeles, 2000.



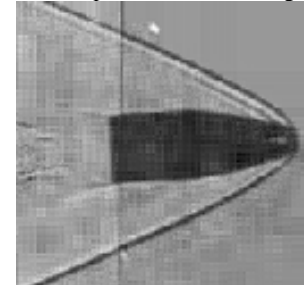
(a) 20% compression and 1 lifting step



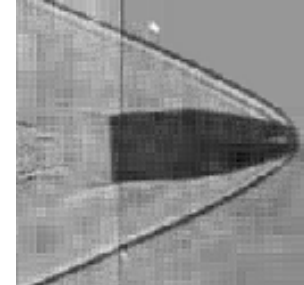
(b) 20% compression and 2 lifting steps



(c) 20% compression and 3 lifting steps

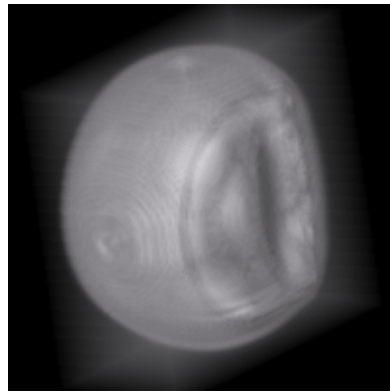


(d) 20% compression and 4 lifting steps

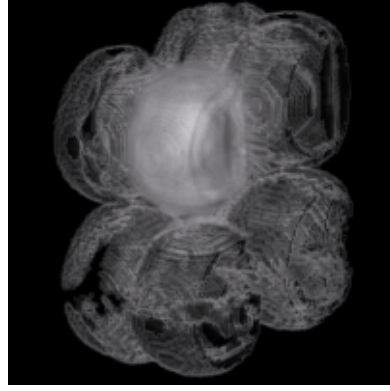


(e) 20% compression and 5 lifting steps

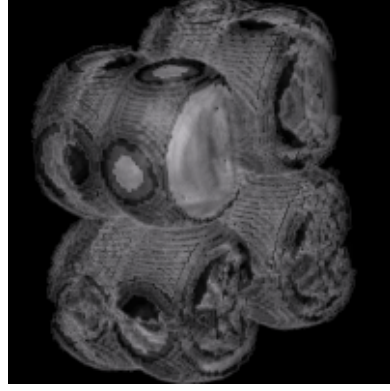
Figure 6: Cubic lifting - 2d shock image



(a) Original explosion image



(b) 3D wavelet transform using TVD wavelet



(c) 3D wavelet transform using cubic wavelet

Figure 7: TVD versus non-TVD in 3D case